J. Serb. Chem. Soc. 69 (10) 783–790 (2004)
JSCS – 3205

UDC 546.65+546.73+547.477:66.094.3
Original scientific paper

Oxidative performance and surface properties of Co-containing mixed oxides having the K_2NiF_4 structure

LAITAO LUO*, HUA ZHONG and XIAOMAO YANG

Institute of Applied Chemistry, Nanchang University, Nanchang, Jiangxi, 330047, P. R. China
(e-mail: Luolaitao@163.com.cn)

(Received 9 December 2003, revised 2 April 2004)

Abstract: The complexed oxides $Nd_{2-x}Sr_xCoO_4$ ($0.4 \le x \le 1.2$) and $LnSrCoO_4$ (Ln = Pr, Nd, Eu) having the K_2NiF_4 structure were synthesized by the citric-acid-complexion method. The results of XRD confirmed that the complexed oxides have the K_2NiF_4 structure. Other phases were found when $x = 0.4$ and $x = 1.2$. The influences of Nd, Pr, Eu on the activities of $LnSrCoO_4$ for CO oxidation and C_3H_8 oxidation were different. The oxidative activities, average crystalline size and lattice distortion of $Nd_{2-x}Sr_xCoO_4$ increased with increasing x value in the oxides. When $x > 0.8$, the lattice distortion decreased with increasing x. The results of O_2–TPD showed that amount of desorption of lattice oxygen over $Nd_{2-x}Sr_xCoO_4$ increased with x, however, the amount of chemidesorption of oxygen decreased. With increasing x, the high-temperature reduction peak in H_2–TPR of $Nd_{2-x}Sr_xCoO_4$ shifted to higher temperatures, however, the low-temperature reduction peak shifted to lower temperatures, which showed that the activity of the lattice oxygen and the thermal stability of $Nd_{2-x}Sr_xCoO_4$ increased with increasing x.

Keywords: rare earths, Co-based mixed oxides, perovskite-like, oxidation.

INTRODUCTION

CO, HC and NO_x emitted from motor vehicles cause severe environmental and health problems.[1,2] In order to eliminate contamination, noble metal catalysts are widely employed at present. However, noble metal catalysts are expensive, so it is of significance to search for low cost alternatives. Perovskite-like A_2BO_4 mixed oxides having the K_2NiF_4 structure consist of alternating layers of ABO_3 perovskite and AO rock salt. They show high catalytic activity for the reactions involved in the after-treatment of motor vehicle exhaust gas, and have recently been studied as new materials.[3,4] At present there are many studies on $LnSrCuO_4$ and $LnSrNiO_4$, but few on $LnSrCoO_4$ (Ln = Ce, Pr, Nd, Eu). In this paper, Co-based mixed oxides $LnSrCoO_4$ and $Nd_{2-x}Sr_xCoO_4$ havihg the K_2NiF_4 structure were prepared by the polyglycol gel method,[5] and their catalytic activities for the oxidization of Co and C_3H_8 were determined.

* Corresponding author.

EXPERIMENTAL

Catalyst preparation

Praseodymium oxide (AR), neodymium oxide (AR), europium oxide (AR), strontium nitrate (AR), cobalt nitrate (AR), polyglycol 20000 (AR) and citric acid (AR) were supplied by the of Shanghai Chemical Reagent Company, China. Cerium carbonate (AR) was supplied by the Institute of Nanchang Rare Earth, China. Nitric acid (AR) and hydrochloric acid (AR) were supplied by the Jiangxi Hongdu Chemical Reagent Factory, China. Series of $LnSrCoO_4$ (Ln = Ce, Pr, Nd, Eu) and $Nd_{2-x}Sr_xCoO_4$ (x = 0.4, 0.6, 0.8, 1.0, 1.2) were prepared by the polyglycol gel method in the desired mole ratio. For example, when x = 0.4, the procedure was as follows: $Nd(NO_3)_3$ (0.5 mol/L, 32 mL), $Sr(NO_3)_2$ (0.5 mol/L, 8 mL) and 6.304 g (0.03 mol) citric acid were mixed with a solution of $Co(NO_3)_3$ (0.5 mol/L, 20 mL). After evaporating the solution to 40 ml at 353 K, polyglycol 20000 (20.0 g) was added under constant stirring. Stirring was continued until a viscous gel was formed. The gel was then evaporated to dryness, and the obtained precursor was calcined at 873 K for 4 h, pelletized and calcined at 1373 K for 10 h. The synthesized pellet was pulverized to *ca*. 0.250 – 0.177 mm.

Characterization

Powder X-ray diffraction (XRD) data were obtained using an X-ray diffractometer (type D8/ADVNCE made in Germany). The analysis conditions were as follows: target, Cu Kα : voltage, 40 kV: current, 40 mA: scan speed, 2º min^{-1}.

Temperature programmed desorption (TPD) experiments were carried out using an automatic Micromeritics 3000 apparatus interfaced to a data station. In each TPD experiment, the samples (0.300 g) for O_2–TPD were first heated from room temperature to 1123 K at a rate of 8 K min^{-1} in a flow of O_2 (40 ml min^{-1}) and then cooled to room temperature. After being He-purged for 1 h, they were heated from room temperature to 1123 K at the same rate. The samples (0.300 g) for CO_2–TPD were first heated from room temperature to 773 K at a rate of 8 K min^{-1} in a flow of He and then cooled to room temperature in a flow of CO_2 (40 ml min^{-1}). After being He-purged for 1 h, they were heated to 773 K at the same rate.

Temperature programmed reduction (TPR) experiments were carried out in the same apparatus as for the TPD experiments. Since water is produced during reduction, the gases out of the reactor were passed through a cold trap before entering the thermal conductivity detector. The samples (0.100 g) were first heated to 1173 K at a rate of 20 K min^{-1} in a flow of N_2 (99.9 %) and then cooled to room temperature. After being 10 % H_2/N_2-purged for 1 h, they were heated to 1173 K at the same rate.

Catalytic activity measurements

The catalytic tests (0.250–0.177 mm, 0.150 g catalyst) were carried out at atmospheric pressure in an automatic Micromeritics flow reactor with a reaction mixture containing CO (5.58 vol.%), O_2 (6.25 vol.%), N_2, total WHSV (10000 h^{-1}) for $CO+O_2$ reaction and C_3H_8 (1.35 vol.%), O_2 (6.75 vol.%), N_2, total WHSV (12000 h^{-1}) for $C_3H_8+O_2$ reaction. The gas composition was analysed before and after the reaction by an in-line gas chromatograph with a thermal conductor detector (TCD) and connected with a computer integrator system. A TDX-01 column was used for CO, N_2 and O_2 and a porapak Q column for C_3H_8 and CO_2. The column temperature was 323 K for both columns and the TCD temperature was 348 K.

RESULTS AND DISCUSSION

Solid characteristics of catalysts

Ganguli[6] proposed that the formation of the K_2NiF_4 structure requires two conditions: a tolerance factor ($t = r_A/r_B$, $1.7 \le t \le 2.4$) and electrovalent equilibrium. The XRD patterns of the $LnSrCoO_4$ (Ln = Ce, Pr, Nd, Eu) mixed oxides showed that Pr, Nd and Eu formed K_2NiF_4-type mixed oxides, whereas, Ce formed an ABO_3 mixed oxide (Fig. 1A), which may be due to an imbalance of the electrovalence caused by the special stability of Ce^{4+} ($4f^0$).

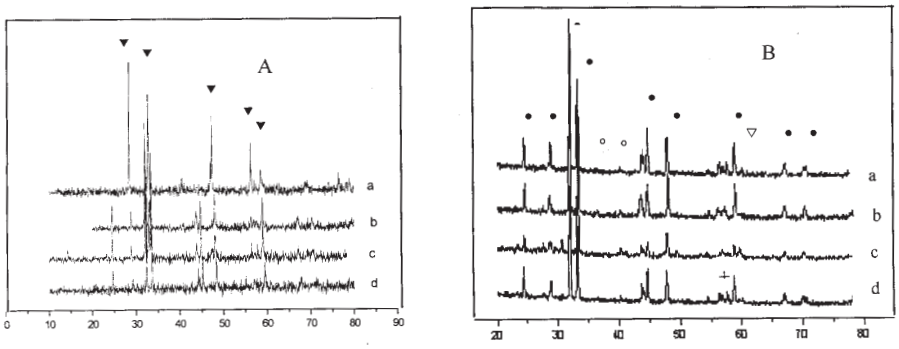

Fig. 1. XRD Patterns of Co-containing complex oxides.A: a: $CeCo_{1-x}Sr_xO_3$; b: $PrSrCoO_4$; c: $NdSrCoO_4$; d: $EuSrCoO_4$; B: $Nd_{2-x}Sr_xCoO_4$ a: $x = 0.4$; b: $x = 0.6$; c: $x = 0.8$; d: $x = 1.2$ ▼: ABO_3 ●: A_2BO_4 ∇: Nd_2O_3, +: $SrCO_3$, o: CoO.

XRD Patterns of $Nd_{2-x}Sr_xCoO_4$ ($x = 0.4, 0.6, 0.8, 1.0, 1.2$) mixed oxides showed that all the $Nd_{2-x}Sr_xCoO_4$ mixed oxides have an K_2NiF_4 structure (Fig. 1B). Among them, when Nd was substituted by a small amount of Sr ($x = 0.4$), the tolerance factor was close to 1.7, a large amount of the Nd and Co in the sample formed K_2NiF_4-type mixed oxides, while a small amount of the Nd and Co formed Nd_2O_3 and CoO. When Nd was substituted by a large amount of Sr ($x = 1.2$), the superfluous Sr cannot enter into an A-site because of its larger ionic radius, which resulted in the formation of $SrCO_3$ and CoO, which was confirmed by XRD.

Oxidative activities of Co-based mixed oxide catalysts

The light-off temperature T_{50} and complete conversion temperature T_{99} of the catalysts (reaction temperatures of 50 % and 99 % conversion, respectively) are assigned as activities. The T_{50} and T_{99} of CO amd C_3H_8 oxidization over $EuSrCoO_4$ catalyst are higher than those of $NdSrCoO_4$ and $PrSrCoO_4$ (Table I). The influence of the three rare earths on CO oxidation was Nd > Pr > Eu.

TABLE I. Effect of the rare earth on the catalytic activity of CO and C_3H_8 oxidation over cobalt complex oxides

Compound	Co oxidation		C_3H_8 oxidation	
	T_{50}/K	T_{99}/K	T_{50}/K	T_{99}/K
$PrSrCoO_4$	527	548	723	823
$NdSrCoO_4$	510	543	743	903
$EuSrCoO_4$	563	588	843	1023

However, their influence on C_3H_8 oxidation was Pr > Nd > Eu. Thus rare earth metals have different effects on the catalytic activities for CO and C_3H_8 oxidization. The catalytic activities of $NdSrCoO_4$ and $PrSrCoO_4$ are very similar, which results from their similar ionic radius and charge. The lower catalytic activities of $EuSrCoO_4$ may result from the lanthanide contraction.

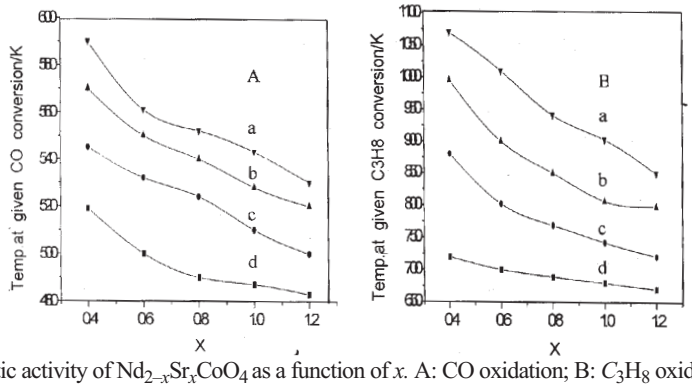

Fig. 2. Catalytic activity of $Nd_{2-x}Sr_xCoO_4$ as a function of *x*. A: CO oxidation; B: C_3H_8 oxidation; conversion: a) 100 %, b) 80 %, c) 50 %, d) 10 %.

As shown in Fig. 2. the T_{50} and T_{99} for CO and C_3H_8 oxidization over $Nd_{2-x}Sr_xCoO_4$ decrease with increasing *x*. The oxidation of C_3H_8 over $Nd_{2-x}Sr_xCoO_4$, because of its stable molecular structure, was more difficult than that of CO.

Effects of Sr on the structure of $Nd_{2-x}Sr_xCoO_4$ mixed oxides

According to the theory of powder X-ray diffraction, the average crystallite size and the lattice distortion at [104] and [110] can be calculated, respectively, by the Scherrer equation

$$L = 0.9\lambda / \beta \cos\theta$$

and

$$\beta^2\cos^2\theta = 4/\pi^2 (\lambda/L)^2 + 32(\varepsilon^2)\sin^2\theta$$

where (β – half width at half maximum, $\lambda = 0.154$ nm, θ – Bragg angle, L – average crystallite size, $(\varepsilon^2)^{1/2}$ – lattice distortion). The calculated values are listed in Table II.

TABLE II. Half width at half maximum, average crystallite size and lattice distortion of $Nd_{2-x}Sr_xCoO_4$ catalysts

Compound	$\beta/10^3$		L/nm		$(\varepsilon^2)^{1/2}/10^3$	
	β_{104}	β_{110}	L_{104}	L_{110}	$(\varepsilon^2)^{1/2}{}_{104}$	$(\varepsilon^2)^{1/2}{}_{110}$
$Nd_{0.8}Sr_{1.2}CoO_4$	7.99	4.87	18.06	29.74	3.42	2.00
$NdSrCoO_4$	8.18	4.96	17.71	29.16	3.49	2.04
$Nd_{1.2}Sr_{0.8}CoO_4$	8.40	5.12	17.18	28.29	3.60	2.10
$Nd_{1.4}Sr_{0.6}CoO_4$	7.41	4.51	19.48	32.08	3.17	1.85
$Nd_{1.6}Sr_{0.4}CoO_4$	6.27	3.82	23.02	37.91	2.69	1.57

β– Half width at half maximum; L– average crystallite size; $(\varepsilon^2)^{1/2}$– lattice distortion

From Table II, it can be seen that Sr has an effect on the structure of $Nd_{2-x}Sr_xCoO_4$ mixed oxides. When $x < 0.8$, the average crystallite size of $Nd_{2-x}Sr_xCoO_4$ mixed oxides at [104] and [110] decrease with increasing *x*, but their lattice distortion increases with in-

creasing x. When $x > 0.8$, the changes of the average crystallite size and the lattice distortion were opposite to the charges when $x < 0.8$, the lattice distortion of $Nd_{2-x}Sr_xCoO_4$ ($x > 0.8$) is bigger than that of $Nd_{2-x}Sr_xCoO_4$ ($x < 0.8$). When $x = 0.8$, a mutation of the lattice distortion was found. It was reported that the B-site ion of A_2BO_4 mixed oxides changes with change of the A-site ion, which causes a distortion of the BO_6 octahedra.[7] The activities of A_2BO_4 mixed oxides are relative to the distortion of the BO_6 octahedra. With increasing distortion of BO_6, the B–O_I bond length increases, however, the B–O_{II} bond length decreases (O_I: the oxygen on the c axes of the crystal lattice, O_{II} the oxygen on the x–y plane of the crystal lattice). The increasing of the movability of oxygen (O_I) is favourable for the oxidation reaction.[8]

Effects of Sr on absorbed oxygen and lattice oxygen of $Nd_{2-x}Sr_xCoO_4$ mixed oxides

The surface oxygen over an oxide catalyst exists in the equilibrium: O_2 (adsorption) $\leftrightarrow$ | O_2^- (adsorption) $\leftrightarrow O^-$ (surface) $\leftrightarrow$ | O^{2-} (surface) $\leftrightarrow O^{2-}$ (lattice). The desorption temperature of O^{2-} (lattice) is higher than those of chemisorbed oxygen (O_2 and O_2^-).[9,10] As shown in Fig. 3, there were two O_2-desorption peaks over the $Nd_{2-x}Sr_xCoO_4$ catalysts, one (≤ 600 K) corresponds to the description of chemisorbed oxygen and the other ≥ 850 K) to the desorption of lattice oxygen. The amount of chemisorbed oxygen decreased with increasing x, however, the amount of lattice oxygen increased. Due to the decrease of the

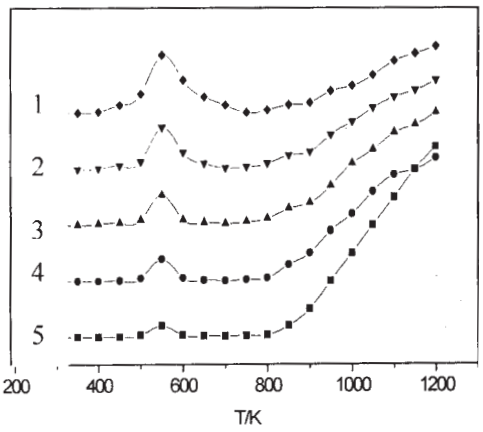

Fig. 3. O_2–TPD Patterns of $Nd_{2-x}Sr_xCoO_4$. 1: $x = 0.4$, 2: $x = 0.6$, 3: $x = 0.8$, 4: $x = 1.0$, 5: $x = 1.2$.

positive charge of the A-site of $Nd_{2-x}Sr_xCoO_4$ catalysts with increasing x, the amount of Co^{2+} (B-site) gradually decreases and, simultaneously, the amount of Co^{3+} gradually increases in order to maintain the electrovalence balance. From the bond energy of adsorption and the electric charge of the atom surface (Fig. 4),[11] it is thought that the chemisorbed oxygen should adsorb on the surface Co^{2+} position or oxygen vacancy. Due to the distortion of the BO_6 octahedra, the Co–O_I bond length is longer than that of Co–O_{II}.[12] The amount of desorbed O_I is connected with Co^{3+}, so the amount of lattice oxygen should be directly proportional to the amount of Co^{3+}. Generally, CO and C_3H_8 are adsorbed on Ni^{3+} over $Ln_{2-x}Sr_xNiO_4$. Hence Ni^{3+} is the active center and lattice oxygen is the active

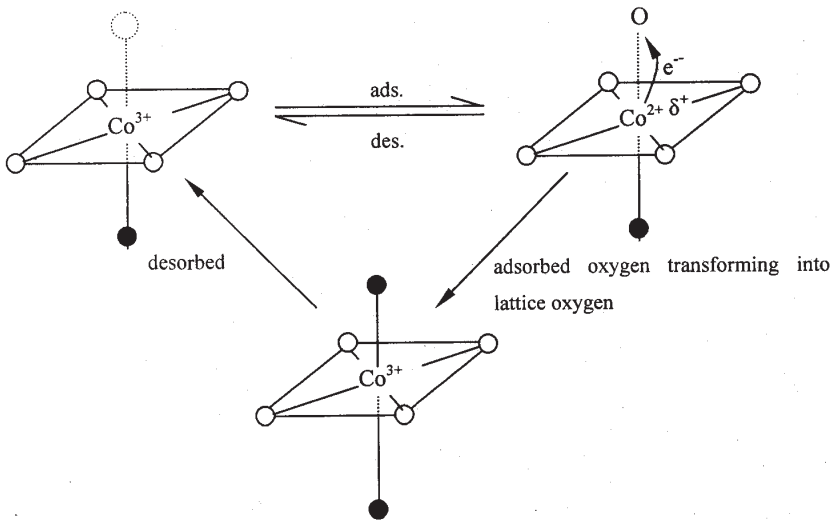

Fig. 4. Scheme of oxygen transformations in the CoO_6 octahedral: O–O_I; ●–O_{II}; ◌– oxygen vacancy.

oxygen species: the chemisorbed oxygen transforms into lattice oxygen to compensate the consumed lattice oxygen.[13] The oxidation mechanism over $Nd_{2-x}Sr_xCoO_4$ is similar to that over $Ln_{2-x}Sr_xNiO_4$. As the amount of Co^{3+}, the desorbed amount of lattice oxygen and the catalytic activities over $Nd_{2-x}Sr_xCoO_4$ all simultaneously increase with increasing x, Co^{3+} can be considered to be the active center and lattice oxygen the active oxygen species.

Effects of Sr on the desorption of CO_2 over $Nd_{2-x}Sr_xCoO_4$ mixed oxides

CO_2 is one of the products of CO and C_3H_8 oxidation. Form Fig. 5, the desorption temperature of CO_2 over $Nd_{2-x}Sr_xCoO_4$ catalysts slightly decrease with increasing x, but the areas under the peaks gradually increase.

Comparing with O_2–TPD (Fig. 3), the desorption temperature of CO_2 is between those of chemisorbed oxygen and lattice oxygen. The adsorption of CO_2 can affect neither the chemisorbed oxygen nor the lattice oxygen. The adsorption of CO_2 and lattice oxygen increases with increasing x, so the number of centers adsorbing CO_2 and chemisorbing ox-

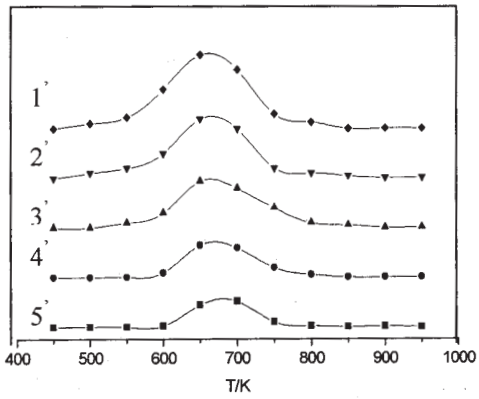

Fig. 5. CO_2–TPD Patterns of $Nd_{2-x}Sr_xCoO_4$. 1: $x = 0.4$, 2: $x = 0.6$, 3: $x = 0.8$, 4: $x = 1.0$, 5: $x = 1.2$.

ygen, as well as the number of lattice oxygens change with changing *x*.

Effects of Sr on reductive property over $Nd_{2-x}Sr_xCoO_4$ mixed oxides

The results of TPR over catalysts $Nd_{2-x}Sr_xCoO_4$ are shown in Table III. These results suggested that there are two H_2-reduction peaks over $Nd_{2-x}Sr_xCoO_4$ mixed oxides, namely, a low temperature peak and a high temperature peak. The temperature of the low temperature peak gradually decreased,

TABLE III. Desorption peak temperature of H_2–TPR over $Nd_{2-x}Sr_xCoO_4$ catalysts

X in $Nd_{2-x}Sr_xCoO_4$	0.4	0.6	0.8	1.0	1.2
Low-temperature peak / K	698	675	654	630	613
High-temperature peak / K	936	967	985	1009	1054

and the temperature of the high temperature peak gradually increased with increasing *x*. As A-site Nd^{3+} and Sr^{2+} could not be reduced by H_2 in the experimental range of temperatures (400–1200 K), it must have been B-site Co ions that were reduced by H_2. The low temperature peak was the reduction of Co^{3+}, *i.e.,*:

$$2Co^{3+} + O^{2-} + H_2 \rightarrow 2Co^{2+} + H_2O$$

whereby the $Nd_{2-x}Sr_xCoO_4$ catalysts kept their original structure. The high temperature peak was the reduction of Co^{2+}, *i.e.,*:[14]

$$Co^{2+} \rightarrow Co^0$$

whereby the K_2NiF_4–type structure was destroyed. Hence, the thermal stability of $Nd_{2-x}Sr_xCoO_4$ catalysts increased with increasing *x*.

CONCLUSION

Perovskite-like $LnSrCoO_4$ (Ln = Pr, Nd, Eu) and $Nd_{2-x}Sr_xCoO_4$ (x = 0.4, 0.6, 0.8, 1.0, 1.2) mixed oxides having the K_2NiF_4 structure were prepared by the polyglycol gel method. The rare earths have certain effects on the catalytic activity of $LnSrCoO_4$. The anount of desorbed lattice oxygen, the amount of Co^{3+} and the catalytic activities of $Nd_{2-x}Sr_xCoO_4$ increased with increasing *x*. When x = 0.8, a lattice distortion mutation of the $Nd_{1.2}Sr_{0.8}CoO_4$ was found.

И З ВО Д

ОКСИДАТИВНА СПОСОБНОСТ И ПОВРШИНСКЕ ОСОБИНЕ МЕШОВИТИХ ОКСИДА КОЈИ САДРЖЕ КОБАЛТ И ИМАЈУ СТРУКТУРУ K_2NiF_4

LAITAO LUO, HUA ZHONG, XIAOMAO YANG

Institute of Applied Chemistry, Nanchang University, Nanchang, Jiangxi, 330047, P. R. China

Синтетисани су мешовити оксиди $Nd_{2-x}Sr_xCoO_4$ ($0,4 \le x \le 1,2$) и $LnSrCoO_4$ (Ln = Pr, Nd, Eu) са структуром која одговара K_2NiF_4 методом комплексирања са лимунском киселином. Резултати XRD потврђују структуру K_2NiF_4, При $x = 0,4$ и 1,2 добијају се друге фазе. Утицаји Nd, Pr и Eu на активност $LnSrCoO_4$ за оксидацију CO i C_3H_8 били су различити. Оксидациона активност, просечна величина критсталита и дисторзија кристалне решетке повећавали су се са повећавањем *x*. Резултати O_2–TPD показали су да се количина кисеоника из решетке изнад $Nd_{2-x}Sr_xCoO_4$ повећавала са повећањем *x*, док се количина хемисорбованог кисеоника смањивала. Повећањем *x* високотемпературни редукциони максимум на H_2–TPR код $Nd_{2-x}Sr_xCoO_4$ померао се ка вишим температурама, док се нискотемпературни редукциони максимум померао ка нижим температурама. Ово показује да се активност кисеоника из решетке и термичка стабилност $Nd_{2-x}Sr_xCoO_4$ повећавају са повећањем *x*.

(Примљенп 9. децембра 2003, ревидирано 2. априла 2004)

REFERENCES

1. Y. N. Armor, *Appl. Catal. B: Environmental* **2** (1992) 256
2. N. Guihaume, S. D. Peter, M. Primet, *Appl. Catal. B: Emvironmental* **10** (1996) 325
3. T. Y. Arakawa, S. I. Tsuchl, Shiolawa, *J. Catal* **74** (1982) 318
4. Y. G. Gangnl, *J. Solid State Chem.* **30** (1979) 358
5. Z. Zhao, X. Yang, Y. Wu, *Science China (Series B)* **40** (1997) 464
6. D. Ganguli, *J. Solid State Chem.* **30** (1979) 353
7. A. K. Ladavos, P. J. Pomonis, *Appl. Catal. A: General* **165** (1997) 73
8. H. Lou, H. Zhen, J. Yang, Z. Yao, X. Yu, W. Du, F Ma, *J. Chin. Rare Earth Soc.* **16** (1995) 107
9. Z. Zhao, X. Yang, Y. Liu, Y. Wu, *J. Science China* **41** (1996) 149
10. G. Shang, X. Ge, H. Zhang, J. Wuli, *Huaxue Xubao* **15** (1999) 568
11. L. Gao, B. Dong, Q. Li, X. Lv, Z. Yu, Y. Wu, *J. Fuel. Chim. Soc.* **22** (1994) 115
12. K. C. C. Kharas, J. H. Lunsford, *J. Am. Chem. Soc.* **111** (1989) 2334
13. S. George, B. Viswanathan, *J. Colloid Chem. Sci.* **95** (1983) 322
14. R. J. Voorhoeve, *Advanced Materials in Catalysis*, Academic Press, New York, 1977, p. 132.